The Toxic Effect of Cu and CuO Nanoparticles on Euplotes Aediculatus

Xiaohuan Zhao
East China Normal University
Zhiwei Gong
East China Normal University
Edgar Pérez
Purdue University
Xilei Gao
East China Normal University
Yiwen Wang
East China Normal University
Xinpeng Fan
East China Normal University
Bing Ni (bni@bio.ecnu.edu.cn)
East China Normal University

Research Article

Keywords: Cu nanoparticles, CuO nanoparticles, Euplotes aediculatus, cytotoxicity

Posted Date: July 7th, 2021

DOI: https://doi.org/10.21203/rs.3.rs-673824/v1

Version of Record: A version of this preprint was published at Microbial Ecology on March 22nd, 2022.
See the published version at https://doi.org/10.1007/s00248-022-01972-3.

Abstract

Toxicology tests were carried out by choosing Cu nanoparticles (CuNPs) and CuO nanoparticles (CuONPs) as experimental materials and *Euplotes aediculatus* as the experimental organism. To investigate the toxicity effect and mechanism of two NPs on *E. aediculatus*, we determined antioxidant enzyme activity and observed morphologic changes using optical and electron microscopes, combined with the Fourier infrared spectrum technique. The results showed that the 24 h-LC_{50} of CuNPs and CuONPs was 0.46 μg/L and 1.24×10^{3} μg/L. The movement ability of cells was decreased and surface cilia gradually shed with CuNPs and CuONPs at 24 h-LC_{50}. In addition, the cell body swelled and finally ruptured. There were varying extents of damage to the nucleus and mitochondria. With CuNPs, disappearance of nucleoli and condensation of chromatin were observed, while the mitochondria were wrinkled in an irregular shape and cristae were partially fractured. With CuONPs, changes of nucleus were not obvious, and the mitochondria were merely irregular. While neither CuNPs nor CuONPs had major effect on the ultrastructure of the membrane, some functional groups were oxidized with CuNPs, e.g. PO_2^-, C-O-C, δ(COH) of carbohydrates. The 24 h-EC_{50}, 48 h-EC_{50} and 72 h-EC_{50} of CuNPs on *E. aediculatus* were 2.10×10^{-3} μg/L, 7.92×10^{-4} μg/L and 2.77×10^{-4} μg/L. The EC_{50} of CuONPs in same period was 7.20 μg/L, 0.86 μg/L and 0.19 μg/L. The above concentration of CuNPs and CuONPs could increase the activities of SOD, CAT and GPx, which were dose-dependent. The above results indicate that CuNPs and CuONPs inhibited reproduction and caused death. CuNPs were more toxic to *E. aediculatus* and more destructive to cell structure. Oxidative stress and destruction to cell structures may be toxic mechanisms. The *E. aediculatus* was more sensitive to CuNPs or CuONPs, and the value of 24 h-LC_{50} was much lower than other organisms, so it can be recommended as an indicator for early monitoring in freshwater environment.

1 Introduction

Nanotechnology is one of the most promising new technologies in the 21st century. At present, nanoparticles (NPs) are widely used in various fields, such as biomedicine (Ediriwickrema and Saltzman, 2015), food processing (Tiede et al., 2008) and energy (Lohse and Murphy, 2012). As NPs are used more and more in industry and general life, they will inevitably enter the ecological environment in the process of production, use and abandonment, thus posing potential threats to the environment and human health (Brumfiel, 2003; Paul et al.,2006; Liu et al., 2019).

Copper is one of the most used metals across many industries, including in particulate matter from power plants, smelters, and metal foundries, and in particles torn from asphalt and rubber tires (Waldron, 1980). Copper nanoparticles (CuNPs) can be used as lubricating oil, conductive coating and catalyst, among other uses (Wen and Li, 2011). Copper oxide nanoparticles (CuONPs) play an important role in the fields of wastewater treatment, coating, sensors and compositing with other materials (Fu et al., 2015). Both have antibacterial properties (Azam et al., 2012; Ramyadevi et al., 2012; Ren et al., 2009), and because of

this, they also have biological toxicity (Manusadzianas et al., 2012; Ostaszewska et al., 2016; Song et al., 2015).

Ramyadevi et al. (2012) studied inhibitory activity of CuNPs in a range of bacteria, including *Staphylococcus aureus* and *Escherichia coli*, and fungus including *Aspergillus flavus* and *Aspergillus niger*. Azam et al. (2012) reported that CuONPs exposed inhibitory effects on both Gram-positive and -negative bacteria. Ren et al. (2009) found that CuONPs had strong activity against *S. aureus* and *E. coli*. This suggests that when CuNPs or CuONPs eventually enter the water environment, they can also attack other single-celled organisms like protozoa. Ostaszewska et al.(2016) studied the acute toxicity of CuNPs to *Acipenser baerii* and found that the 96 h-LC_{50} value was (1.41 ± 0.24) mg/L. Toxicity effects induced by CuNPs on five cladoceran species (*Daphnia magna*, *D. pulex*, *D. galeata*, *Ceraphaphnia dubia*, *Chydorus sphaericus*) can cause death in all of them (Song et al., 2015). Research has shown that 96 h-LC_{50} of *Nitellopsis obtusa* was (2.8–4.3) mg/L with CuONPs, 24h-LC_{50} of *Thamnocephalus platyurus* was (8.5–9.8) mg/L, and 24h-LC_{50} of *Brachionus calyciflorus* was (0.24–0.39) mg/L (Manusadzianas et al., 2012). In addition, some studies have shown that organisms take in NPs and then affect high-nutrient organisms through the food chain (Werlin et al., 2010; Ferry et al., 2009; Lewinski et al., 2011; Bouldin et al., 2008). However, few reports have compared the toxicity of CuNPs and CuONPs. And few studies have directly demonstrated the destruction of cellular structures by CuNPs or CuONPs.

Protozoa, the most primitive, lowest and simplest eukaryotic animals, play a key role in energy flow and material circulation (Klaus et al., 2007). They respond rapidly to changes in the outside world and can be useful indicators (Patterson, 1992). *Euplotes* species belong to the phylum of ciliate protozoa. They are widely distributed in nature and easily accessible (Klaus et al., 2007). They are easy to grow in the laboratory, and their cell cycle is simple. Their membrane can make direct contact with NPs and heavy metals, which makes them sensitive to the pollutants (Liu et al., 2010; Vaiopoulou and Gikas, 2012). As a result, their cellular responses reflect environmental changes in a timely manner, and their responses to the environment are more convincing than those of prokaryotes (Liu et al., 2010; Nadtochenko et al., 2005; Nadtochenko et al., 2006).

In our study, *Euplotes aediculatus* was selected as the experimental organism and CuNPs and CuONPs were selected for toxicological testing to preliminarily explore the toxic effects of the two NPs on *E. aediculatus*. The toxicity of CuNPs and CuONPs was compared by measuring the semi-lethal concentration. Changes in cell morphology were observed using optical microscopy and scanning electron microscopy (SEM). The ultrastructure of cells was inspected using transmission electron microscopy (TEM). Attenuated total reflection Fourier transform infrared spectroscopy (ATR-FTIR) was used to measure the oxidative damage to the cell membranes, and enzyme activity was used to evaluate cell activity.

2 Materials And Methods

2.1 Cell culture

E. aediculatus was taken from a closed freshwater pond in Zizhu Garden, Minhang District, Shanghai. After separation, wheat fermentation was used for pure culture in incubator (temperature: 25 ℃, humidity: 76% RH). Before the experiment, the cells at the growth equilibrium stage were obtained and washed with ultrapure water 2–3 times.

2.2 Preparation of NPs suspensions

NPs were purchased from Aladdin. They were mixed with the cultured water and depolymerized by ultrasound (SCQ-70). The morphology and size of NPs were characterized using a transmission electron microscope (TEM, HT-7700) and dynamic light scattering (DLS, Zetasizer Nano ZS90).

2.3 Determination of 24 h-LC_{50} and 24 h-EC_{50}, 48 h-EC_{50}, 72 h-EC_{50}

Three replicates were set for each concentration. Every replicate contained 200 μL suspension and 10 cells. The control test was performed without toxicant. The test was conducted in incubator. The mortality in each group was observed and recorded after 24 h to estimate the median lethal concentration (LC_{50}). The mortality in each group was observed and recorded after 24, 48 and 72 h to estimate the median effect concentration (EC_{50}).

2.4 Cell growth curve

The different EC_{50} above were taken as experimental concentrations, with five replicates in each group. Only one active cell was added to 200 μL culture water for control or various concentrations suspension with NPs. Cell number in each group was recorded, with 20 μL of wheat fermentation added daily. The experiment lasted for 21 days.

2.5 Enzymes activity assay

The different EC_{50} above were taken as experimental concentrations, with three replicates in each group. Cell were filtered and collected into a petri plate with 200 μL culture water for control or suspensions. Cells were collected to determine superoxide dismutase (SOD), glutathione peroxidase (GPx) and catalase (CAT) after 24 h. For details, refer to the SOD, GPx and CAT test kit instructions (purchased from the Nanjing Jiancheng Bioengineering Institute).

2.6 Observation of living cells

The 24 h-LC_{50} was used as the experimental concentration. Samples were prepared with treatment times of 1.0, 1.5, 2, 2.5 and 3 h. Living cells from control and experimental groups were isolated and observed in vivo by microscopy (Nikon DS-Ri2).

2.7 SEM observation

The 24 h-LC_{50} was used as the experimental concentration. Samples were prepared with treatment times of 0.5, 1.0, 1.5, 2 and 3 h. Cells were collected and fixed using 4% osmium tetraoxide (OsO4) for 10 min.

After washing with buffer, the cells were then dehydrated in gradient concentration of ethanol (30%,50%, 70%, 80%, 90%, 95% and 100%), critical-point dried, and sputter coated with platinum. Samples were observed by SEM (Hitachi, S4800).

2.8 TEM observation

The 24 h-LC_{50} was used as the experimental concentration. Samples were prepared with treatment time at 2 h. Cells were fixed in a 1:1 mixture of 2.5% glutaraldehyde and 2% OsO4 for 30 min. After washing with buffer, cells were post-fixed in 1% O_SO_4 for 1 h. They were then dehydrated in a graded acetone series, embedded with Epon 12 and polymerized at 37°C for 16 h, 45°C for 24 h and 60°C for 48 h. Ultrathin sections were cut with a diamond knife and then stained with uranyl acetate and lead citrate. The sections were observed by TEM (Hitachi, HT-7700).

2.9 ATR-FTIR

Cells in control and the experimental group (24 h-LC_{50}) were filtered and collected. Samples were pre-frozen for 12 h, vacuum freeze-dried, and measured by FTIR spectroscopy (NEXUS 670).

2.10 Statistical analysis

SPSS (version 23.0 for Windows) software was used for the statistical analysis. The mean was compared by T-test and one-way anova to determine whether significant variation existed between the treatments. $P < 0.05$ was considered statistically significant. GraphPad Prism7 software was used to plot.

3 Results

3.1 Characterization of CuNPs and CuONPs

The morphologies of CuNPs and CuONPs were verified by TEM, which showed that they were circular and the particle sizes were about 30 nm. CuNPs had a wider size distribution, and CuONPs had a more uniform size. Both possessed negative zeta potential (-28.18 mV, -30.10 mV) and were relatively stable in solution. This meant that the NPs used in this experiment were suitable for toxicity testing.

In TEM images of CuNPs (A) and CuONPs (C), both were circular and the particle sizes were about 30 nm. Zeta potentials of CuNPs (B) and CuONPs (D) were − 28.18 mV and − 30.10 mV respectively.

3.2 Toxicity tests of NPs on *E. aediculatus*

3.2.1 Determination of 24 h-LC_{50}

The mortality of cells in each group was calculated after 24 hours. The regression curve of acute toxicity of CuNPs and CuONPs is shown in Fig. 2. The mortality rate was linear with the logarithm of the concentration of NPs. Regression equation of CuNPs was Y = 0.205*X + 0.57, R^2 = 0.9856, LC_{50} = 0.46

μg/L. Regression equation of CuONPs was Y = 0.4184*X − 0.794, R^2 = 0.9855, LC_{50} = 1.24×10^3 μg/L. It was showed that CuNPs were more toxic to *E. aediculatus.*

3.2.2 Determination of 24 h-EC_{50}, 48 h-EC_{50}, 72 h-EC_{50}

The reproduction rate of the two NPs to cells was measured in a certain time and concentrations range. As pictured above, there was a linear relationship between the reproduction rate and the logarithm of the concentrations of NPs. The EC_{50} values of CuNPs were lower than those of CuONPs in the same period. The longer the treatment time, the lower the EC_{50} value of the two NPs was.

Table 1
EC_{50} values of the two NPs in different treatment time on *E. aediculatus*

Treatment time(h)	CuNPs (μg/L)			CuONPs (μg/L)		
	EC_{50}	Regression equation	R^2	EC_{50}	Regression equation	R^2
24	2.10×10^{-3}	Y = 0.9132*X + 2.945	0.9954	7.20	Y = 0.4171*X + 0.1423	0.9814
48	7.92×10^{-4}	Y = 0.6984*X + 2.666	0.9888	0.86	Y = 0.6822*X + 0.5432	0.9856
72	2.77×10^{-4}	Y = 0.6224*X + 2.714	0.9859	0.19	Y = 0.37*X + 0.7637	0.9961

3.3 Effect of NPs on cell growth curve

The growth curve of the control group was S-shaped, as shown in Fig. 3. The CuNPs group with a concentration of 24 h-EC_{50} had the strongest inhibition on cell growth. The number of cells barely changed. At a concentration of 48 h-EC_{50}, the cells stopped reproducing after 13 days. The concentration of 72 h-EC_{50} had the weakest inhibition on cell proliferation. The CuNPs group also showed similar dose-dependent changes. The inhibition effect of CuNPs was stronger than that of CuONPs.

3.4 Enzyme activity assay

Compared with the control group, the activities of T-SOD, GPx and CAT were higher in the experimental groups with different concentrations of CuNPs (Fig. 4A) and CuONPs (Fig. 4B), and the difference was statistically significant (P< 0.05). With the increase of treatment concentration, the activity of all three enzymes increased, which was dose-dependent. The activities of T-SOD, GPx and CAT in the CuNPs groups were higher than those in the CuONPs in the same period (Fig. 4C). CuNPs can cause more intense oxidative stress.

Figure 4 shows the effects of different concentrations of CuNPs (A) and CuONPs (B) on enzyme activit, and the comparison of the activity of the same enzyme between the two NPs (C).

3.5 Morphogenetic observation

3.5.1 Observation of living cells

E. aediculatus was about 130–150 μm long × 70–90 μm wide and ellipsoidal, with full endoplasm (Fig. 5A). Cells possessed ventral ciliary organelles integrally. They could swim freely through the movement of the cilia.

After treatment with CuNPs, the movement state and morphology of the cells changed to various degrees with treatment time. The cells whirled in place, and the cirri quivered violently (Fig. 5B, C). After that, the cell movement weakened, and the cilia wobbled weakly until they were still and died (Fig. 5D-F). A few small vacuoles appeared in the cell body (Fig. 5B), which gradually fused and expanded (Fig. 5C, D). The cell body was swollen and deformed into a ball, and the endoplasm of cell lysis flowed out (Fig. 5E, F).

Similar to the CuNPs groups, the changes to the cell in movement state and morphology were also observed in CuONPs groups. There was no significant change in motion state and morphology at first (Fig. 5G). Many small vacuoles appeared in the cells (Fig. 5G). The cilia quivered intensely, and several small vacuoles gradually fused into large vacuoles (Fig. 5H, I). The movement of cilia gradually weakened, and then cells were stationary (Fig. 5J-L). The vacuoles filled the whole cell, and the cell swelled into a ball (Fig. 5J, K). The cell membrane ruptured, and cell death occurred (Fig. 5L).

A: Control. B-F: Morphological changes in CuNPs group with 24 h-LC_{50}. B: Cells treated for 1.0 h showed vacuoles. C: Vacuoles fused for 1.5 h. D: The vacuoles continued to increase and the cell body expanded for 2.0 h. E: The cell swelled spherically. F: The cell cleaved and the endoplasm flowed out and spread around after 3.0 h. G-I: Morphological changes in CuONPs group with 24h-LC_{50}. G: Cells treated for 0.5h showed small vacuoles. H: Small vacuoles fused for 1.0 h. I: the vacuoles continued to grow for 1.5 h. J: Cells began to swell for 2.0 h. K: The cell was spherical after 2.5 h. L: Cells were gradually lysed after 3.0 h. A-H: Scale bars = 50 μm.

3.5.2 SEM observation

SEM images showed that the control cell possessed ventral ciliary organelles integrally. Front-ventral cirri (FVC), transverse cirri (TC), caudal cirri (CC) and left marginal cirri (LMC) were distributed at specific locations on the cell surface, which constituted the unique ciliary pattern of *E. aediculatus*. The adoral zone of membranelles (AZM) was located on the left side of the FVC, accounting for 2/3 of the body. The undulating membrane (UM) was located on the right side of the base of AZM (Fig. 6A). The cell morphology and cilium structure varied with the treatment time of NPs. With 24h-LC_{50} as the treatment concentration, the cell volume did not change significantly when treated with CuNPs for 0.5-1.0 h. The LMC and CC were completely shed, and the kinetosome was partially shed (Fig. 6B, I). FVC and TC were partially shed (Fig. 6B, G, H). After treatment for 2.0 h, cell volume decreased slightly, FVC and TC shed

increasingly, and the cilia of the collar part of AZM (AZM-C) and lapel part of AZM (AZM-L) began to drop off (Fig. 6C, J). The cell was spherical, leaving only cilia of AZM after 3.0 h (Fig. 6D, E, F).

A: Control. B: Morphological changes in CuNPs group with 24h-LC_{50} during treatment of 0.5-1.0 h. Arrows from top to bottom showing the shedding of FVC and LMC. C: FVC and partial AZM shed for 2.0 h. D-F: Cell was spherical after 2.5-3.0h. The cell expanded in a spherical shape, leaving only cilia of AZM. G-J: Partial enlargement of FVC, TC, LMC and AZM. Abbreviations: FVC = front-ventral cirri, LMC = left marginal cirri, AZM = adoral zone of membranelles, TC = transverse cirri, CC = caudal cirri. Scale bars = 50 μm (ACDF), 40 μm (BE), 10 μm (GH), 1 μm (IJ).

Cells treated with 24h-LC_{50} CuONPs manifested similar changes. During the first 0.5 h, there was no significant change in cell body size. FVC and CC began to shed (Fig. 7A, F, G). After another 0.5 h, the LMC and CC were completely shed (Fig. 7B), the FVC was shed more (Fig. 7B, H), and the TC have begun to shed (Fig. 7I). At 2.0 h, the FVC was completely shed, and the TC was shed more (Fig. 7C, J, K). The cells were spherical, leaving only cilia of AZM (Fig. 7D, E) for 3.0 h and after.

A: Morphological changes in CuONPs group with 24h-LC_{50} for 0.5 h. Arrows from top to bottom show the shedding of FVC and CC. B: FVC, CC and LMC shed more (Arrows from top to bottom). C: FVC shed totally after 2.0 h. D, E: Cell was spherical within 2.5-3.0h, leaving only cilia of AZM. F-K: Partial enlargement of FVC, CC, FVC, TC, FVC and TC. Scale bars = 50 μm (ABCD), 40 μm (E), 10 μm (FH), 2 μm (GIJK).

3.6 TEM observation

The membrane of *E. aediculatus* was intact and complete (Fig. 8A), composed of the plasma membrane and the outer and inner membranes of the alveolus (Fig. 8B). The microtubules below the cortex were arranged in a triangle pattern (Fig. 8C). The cytoplasm was dense, and mitochondria were concentrated mainly under the cortex (Fig. 8A-C, E). The mitochondria of the control cell were round or oval and composed of a double-layer membrane, with the inner membrane folded inward into cristae (Fig. 8A-C). The macronucleus was clearly demarcated in the control cell. Nucleoli and chromatin were evenly distributed in the macronucleus (Fig. 8D).

A: The complete membrane and the mitochondria below it. B: The membrane structure included plasma membrane, outer membrane and inner membrane of the alveolus (arrows). C: The microtubules below the cortex were arranged in a triangle pattern (arrows). D: Macronucleus. Nucleoli and chromatin were distributed in the macronucleus. E: Mitochondria in the cortex and cytoplasm.

Structure of membrane was relatively intact without obvious damage in experimental groups with CuNPs(Fig. 9A) or CuONPs (Fig. 10A). Mitochondria were wrinkled and deformed (Fig. 9B), some structures were seriously damaged, and the cristae were fractured because of CuNPs (Fig. 9C). While the morphology of the mitochondria changed significantly to an irregular shape, the cristae did not break in the group of CuONPs (Fig. 10B, C). With CuNPs, the nucleoli disappeared and the chromatin

condensation shrank significantly (Fig. 9E). However, there was no significant change in the nucleus with CuONPs (Fig. 10E).

A: The intact membrane. B: Mitochondria were wrinkled and deformed. C: The cristae in Mitochondria were fractured. D, E: Changes in morphology and structure of the macronucleus. The nucleoli disappeared, and the chromatin condensation shrank significantly.

A: The intact membrane. B, C: Mitochondria were wrinkled, and their morphology changed to an irregular shape. The cristae did not break. D, E: Macronucleus. No significant change in the nucleus.

3.7 ATR-FTIR

As shown in Fig. 11, the most prominent peaks, at 2360, 1646 and 1543 cm^{-1}, were CO_2, amide Ⅰ and amide Ⅱ, respectively, in the control group. The peaks of *E. aediculatus* in the spectra refer to supplementary material 1 (S1 ATR-FTIR peaks of *E. aediculatus* in the spectra). Peaks at 2925, 2856, 1457 and 1083 cm^{-1} were prominent as well. The first three belonged to C-H bonds, while the latter was $v_s(PO_2\text{-})$.

The relatively gentle peaks were 1243, 1050 and 1020 cm^{-1}, corresponding to $v_a(PO_2\text{-})$, δ(COH) of carbohydrates and C-O-C, respectively. With the two NPs, some of the groups weakened or disappeared, and new groups were produced. Functional groups of C-H, amide Ⅰ, amide Ⅱ, $v_a(PO_2^-)$ and $v_s(PO_2^-)$ were weakened, δ(COH) of carbohydrates and C-O-C disappeared in the group of CuNPs. Meanwhile, the $-COO^-$ str. group was added at 1393 cm^{-1}. However, CuONPs had less effect on the above groups, and only the $-COO^-$ str. group was added, at 1412 cm^{-1}.

4 Discussions

4.1 Comparison of toxicity of CuNPs and CuONPs against *E. aediculatus*

There have been many studies on the toxicity of CuNPs and CuONPs, but few that compare their toxicity. Ostaszewska et al. (2016) studied the acute toxicity of CuNPs to *Acipenser baerii* and found that the 96 h-LC_{50} value was (1.41 ± 0.24) mg/L. Song et al. (2015) studied toxicity effects induced by CuNPs in different sizes (25 nm, 50 nm, 100 nm, 500 nm) on five cladoceran species (*Daphnia magna*, *D. pulex*, *D. galeata*, *Ceraphaphnia dubia*, *Chydorus sphaericus*) and found that all 48 h-LC_{50} values were greater than 0.001 mg/L. Another study showed that 96 h-LC_{50} of *Nitellopsis obtusa* was (2.8–4.3) mg/L with CuONPs, 24h-LC_{50} of *Thamnocephalus platyurus* was (8.5–9.8) mg/L, and 24h-LC_{50} of *Brachionus calyciflorus* was (0.24–0.39) mg/L (Manusadzianas et al., 2012). In a comparative study on toxicity of CuNPs and CuONPs, Midander et al. (2009) found that CuNPs had a wider cytotoxicity. Kovriznych et al. (2013) showed 48 h-LC_{50} values of CuNPs on adult zebrafish and egg of 4.2 and 24.0 mg/L, respectively, and 48 h- LC_{50} values of CuONPs on adult zebrafish and egg of 400 and 960 mg/L, respectively. So far,

there is no study on the comparative toxicity of CuNPs and CuONPs to protozoa. In our study, the LC_{50} and EC_{50} values of CuNPs were lower than those of CuONPs, and the toxicity of CuNPs to *E. aediculatus* was stronger. In addition, our study also found that the *E.aediculatus* was sensitive to CuNPs (24 h-LC_{50} value was 0.46 μg/L) or CuONPs (24h-LC_{50} value was 1.24 mg/L), and the 24 h-LC_{50} values were much lower than other organisms, which can be recommended as an indicator for early monitoring in freshwater environment.

4.2 Mechanism of toxicity

4.2.1 Oxidative stress in cell

Cells produce a little reactive oxygen species (ROS) under normal conditions. ROS is cleared by the antioxidant defense system, and the metabolism is in a dynamic state of balance. NPs can stimulate cells to produce more ROS, exceeding their ability for cell clearance, which requires the antioxidant system to react (Franco et al., 2006; Liu et al., 2020). The system consists of antioxidant enzymes and antioxidants. The involvement of enzymes, including SOD, CAT and GPx, is an important defense mechanism to protect organisms from oxidative stress (Kim et al., 2011). SOD dismutates superoxide anion radical $O^{2-\cdot}$ into H_2O_2, which is transformed into H_2O by CAT. ROS can be effectively eliminated by coordinating SOD and CAT (Geracitano et al., 2004). Glutathione (GSH), an antioxidant, plays a critical role in detoxification pathways of electrophiles such as copper (Anderson and Luo, 1998), and it is the substrate of GPx (Kim et al., 2011). GPx is also an important enzyme to catalyze H_2O_2 (Kim et al., 2011). Kim et al. (2011) proved that copper could increase the expression of GPx gene in *E. crassus.* Research has shown that CuNPs increased the ROS in renal tissues and decreased the levels of biomarkers (SOD, CAT, GST and GPx activity) related to oxidative stress (Sarkar et al., 2011). Maybe the antioxidant system was destroyed due to the stronger toxicity of CuNPs. Wang et al. (2012) proposed that mitochondria in human lung epithelial cells depolarized, which was induced by ROS production to further enhance oxidative stress after CuONPs entered. Three kinds of antioxidant enzymes were all increased in treated groups with two NPs, and oxidative stress reaction was produced in *E. aediculatus.* Lin et al. (2009) showed that CuNPs had more active chemical properties and more active sites, so it was easier to produce free radical $O^{2-\cdot}$ and ROS, which could increase the oxidative pressure of cells, further causing lipid peroxidation and leading to cell membrane damage. According to other studies, the outer layer of CuNPs had surface oxides such as Cu_2O and CuO, which allowed for easier extraction of Cu^{2+}. When organisms produced too much superoxide such as $O^{2-\cdot}$ or contained reductants, they could reduce Cu^{2+} to Cu^{+}. Cu^{+} could then catalyze H_2O_2 to generate hydroxyl radicals (Bremner, 1998; Gaetke and Chow, 2003). CuONPs are composed of CuO, with a single component and slightly weaker chemical properties than CuNPs. So it is speculated that these may be less toxic to cells.

4.2.2 Damage to cell membrane, mitochondria, and nuclei

NPs penetrated cells by changing the permeability of cell membranes and reacted with intracellular substances to cause cytotoxicity (Han et al., 2012). Liu et al. (2010) observed that NPs destroyed the

membrane so that it lost selective permeability, and its permeability increased. Lv (2019) showed that TiO_2NPs seriously damaged the ultrastructure of the membrane in *Pseudourostyla cristata*. Nevertheless, AgNPs caused no obvious damage to the membrane of *E. aediculatus* (Ren, 2016). In our study, ultrastructural results exhibited no damage in the membrane of *E. aediculatus*. However, changes in the chemical composition of the cell membrane was detected by ATR-FTIR. Amide groups, C-H, P = O, δ(COH) of carbohydrates and C-O-C groups are the main functional groups that constitute cell membrane components, i.e. proteins, phospholipids and glycoproteins (Kiwi and Nadtochenko, 2005). Amide groups are linked to hydrophobic ends and exposed to the environment, so the peaks of these are most significant. Decay of amide groups suggested that the outer hydrophobic ends were easily oxidized with CuNPs. Changes in $v_a(PO_2^-)$ and $v_s(PO_2^-)$ indicated the destruction of lipid (Kinder et al., 1997; Nadtochenko et al., 2005). Decreases in δ(COH) of carbohydrates and C-O-C groups indicated damage to polysaccharides and glycoproteins (Nadtochenko et al., 2005). The presence of the -COO- str group was due to the unsaturated aldehydes formed during the decomposition of peroxides in hydroperoxides or lipids, as well as the C = O stretched bonds in the formation of carboxyl groups (Gericke and Huehnerfuss, 1995). While CuNPs or CuONPs had little effect on the ultrastructure of the membrane, some functional groups of membrane were oxidized at molecular level. It has been further proven that cells produce oxidative stress in response to exogenous stimulus factors.

Many studies have shown that CuNPs or CuONPs can damage cell structures such as mitochondria and nuclei. CuNPs and CuONPs can cause DNA damage in human lung cells (Midander et al., 2009). Studies have also shown that CuNPs broke the DNA chains in rat ovaries and promoted cell apoptosis (Yang et al., 2017). The expression of cell cycle checkpoint protein p53 and DNA damage repair proteins Rad51 and MSH2 was up-regulated with CuONPs (Ahamed et al., 2010). NPs damaged the chromosomes, causing genetic changes and DNA damage (Kisin et al., 2011). In our study, CuNPs and CuONPs caused damage to the nucleus. This was consistent with previous studies. Destruction caused by CuNPs was more serious. Lei et al. (2008) proposed that CuNPs could induce necrosis of liver cells and renal tubules and failure of mitochondrial function. Another study showed that mitochondrial dysfunction and oxidative damage were the main causes of the toxicity of CuNPs in rats (Lei et al., 2015). CuONPs could decrease mitochondrial membrane potential, upregulate the apoptosis gene and result in apoptosis in human hepatocytes (Siddiqui et al., 2013). Sankar et al. (2014) found that cell apoptosis with CuONPs was mediated by the production of ROS, involving the destruction of mitochondrial membrane potential in A549 cells. ROS generation and GSH reduction lead to mitochondrial dysfunction (Chen and Schluesener, 2008). Some scholars believed that cells produced oxidative stress with NPs, they mainly attacked the cristae of mitochondria, affected the electron transport chain, produced much ROS, and interfered with the synthesis of ATP (AshaRani et al., 2009). In this study, the morphology and structure of mitochondria changed and ruptured significantly with the two NPs, worse with CuNPs than with CuONPs. The above phenomena were consistent with the results from toxicology experiments that the two most important toxic mechanisms with CuNPs and CuONPs were the destruction of nucleus and the mitochondrial dysfunction mediated by the production of ROS.

5 Conclusions

The toxic effect of CuNPs and CuONPs on *E. aediculatus* was studied, and the mechanism was preliminarily investigated for the first-time using enzyme activity determination, electron microscope, ATR-FTIR and other methods. CuNPs and CuONPs inhibited reproduction and caused cell death, mainly by stimulating oxidative stress and damaging cell structures such as mitochondria and nucleus. The toxic effect of CuNPs on *E. aediculatus* was stronger than that of CuONPs.

Declarations

Acknowledgements

This work was supported by the National Natural Science Foundation of China (No.31672249). We thank the ECNU Multifunctional Platform for Innovation (004).

Funding: This work was supported by the National Natural Science Foundation of China (No.31672249).

Conflicts of interest/Competing interests: We declare that we have no financial and personal relationships with other people or organizations that can inappropriately influence our work, there is no professional or other personal interest of any nature or kind in any product, service and/or company that could be construed as influencing the position presented in, or the review of, the manuscript entitled, “The toxic effect of Cu and CuO nanoparticles on *Euplotes aediculatus*”.

Availability of data and material: The experimental materials and data are true and reliable, and have not been disclosed to other journals except this journal.

Code availability Not applicable

Authors' contributions: Every author performs his own duties and undertakes certain tasks in this study, and the order of the authors is fairly distributed according to the workload.

Additional declarations for articles in life science journals that report the results of studies involving humans and/or animals Not applicable

Ethics approval: Not applicable

Consent to participate: Informed consent was obtained from all individual participants included in the study.

Consent for publication: The participant has consented to the submission of the case report to the journal.

References

1. Ahamed M, Siddiqui MA, Akhtar MJ, Ahmad I, Pant AB, Alhadlaq HA (2010) Genotoxic potential of copper oxide nanoparticles in human lung epithelial cells. Biochem Biophys Res Commun 396:578–583
2. Anderson ME, Luo JL (1998) Glutathione therapy: from prodrugs to genes. Semin Liver Dis 18:415–424
3. AshaRani PV, Low KMG, Hande MP, Valiyaveettil S (2009) Cytotoxicity and genotoxicity of silver nanoparticles in human cells. ACS Nano 3:279–290
4. Azam A, Ahmed AS, Oves M, Khan MS, Memic A (2012) Size-dependent antimicrobial properties of CuO nanoparticles against Gram-positive and -negative bacterial strains. Int J Nanomedicine 7:3527–3535
5. Bouldin JL, Ingle TM, Sengupta A, Alexander R, Hannigan RE, Buchanan RA (2008) Aqueous toxicity and food chain transfer of quantum dots™ in freshwater algae and Ceriodaphnia dubia. Environmental Toxicology Chemistry 27(9):1958–1963
6. Bremner I (1998) Manifestations of copper excess. Am J Clin Nutr 67:1069S–1073S
7. Brumfiel G (2003) Nanotechnology: A little knowledge. Nature 424:246–248
8. Chen X, Schluesener HJ (2008) Nanosilver: a nanoproduct in medical application. Toxicol Lett 176:1–12
9. Ediriwickrema A, Saltzman WM (2015) Nanotherapy for Cancer: Targeting and Multifunctionality in the Future of Cancer Therapies. ACS Biomaterials Science & Engineering. 1, 64–78
10. Ferry JL, Craig P, Hexel C, Sisco P, Frey R, Pennington PL, Fulton MH, Scott IG, Decho AW, Kashiwada S, Murphy CJ, Shaw TJ (2009) Transfer of gold nanoparticles from the water column to the estuarine food web. Nat Nanotechnol 4:441–444
11. Franco JL, Trivella DB, Trevisan R, Dinslaken DF, Marques MR, Bainy AC, Dafre AL (2006) Antioxidant status and stress proteins in the gills of the brown mussel Perna perna exposed to zinc. Chem Biol Interact 160:232–240
12. Fu X, Ge T, Zhu F, Xue Y, Lin D (2015) Review of environmental impact and ecotoxicological effects of copper oxide nanoparticles. Jiangsu Agricultural Sciences. 340–344
13. Gaetke LM, Chow CK (2003) Copper toxicity, oxidative stress, and antioxidant nutrients. Toxicology 189:147–163
14. Geracitano LA, Bocchetti R, Monserrat JM, Regoli F, Bianchini A (2004) Oxidative stress responses in two populations of Laeonereis acuta (Polychaeta, Nereididae) after acute and chronic exposure to copper. Mar Environ Res 58:1–17
15. Gericke A, Huehnerfuss H (1995) Investigation of Z- and E-unsaturated fatty acids, fatty acid esters, and fatty alcohols at the air/water interface by infrared spectroscopy. Langmuir 11:225–230
16. Han S, Li Q, Xia T, Zhong Z, Guo J (2012) Research on Toxicity of Medical Metal and Metallic Oxides Nanomaterials. Acta Biophysica Sinica. 805–814

17. Kim S, Jung M, Lee Y (2011) Effect of heavy metals on the antioxidant enzymes in the marine ciliate Euplotes crassus. Toxicology Environmental Health Sciences 3:213–219
18. Kinder R, Ziegler C, Wessels JM (1997) Gamma-irradiation and UV-C light-induced lipid peroxidation: a Fourier transform-infrared absorption spectroscopic study. Int J Radiat Biol 71:561–571
19. Kisin ER, Murray AR, Sargent L, Lowry D, Chirila M, Siegrist KJ, Schweglerberry D, Leonard S, Castranova V, Fadeel B (2011) Genotoxicity of carbon nanofibers: are they potentially more or less dangerous than carbon nanotubes or asbestos. Toxicology Applied Pharmacology 252:1–10
20. Kiwi J, Nadtochenko V (2005) Evidence for the mechanism of photocatalytic degradation of the bacterial wall membrane at the TiO_2 interface by ATR-FTIR and laser kinetic spectroscopy. Langmuir 21:4631–4641
21. Klaus H, Norbert H, Renate R (2007) Protistology. China Ocean University Press
22. Kovriznych JA, Sotnikova R, Zeljenkova D, Rollerova E, Szabova E, Wimmerova S (2013) Acute toxicity of 31 different nanoparticles to zebrafish (Danio rerio) tested in adulthood and in early life stages comparative study. Interdiscip Toxicol 6:67–73
23. Lei R, Ding R, Yang B, Wang Q, Wu C (2015) Mitochondrial dysfunction and oxidative damage in the liver and kidney of rats following exposure to copper nanoparticles for five consecutive days. Toxicology Research 4(2):351–364
24. Lei R, Wu C, Yang B, Ma H, Shi C, Wang Q, Wang Q, Yuan Y, Liao M (2008) Integrated metabolomic analysis of the nano-sized copper particle-induced hepatotoxicity and nephrotoxicity in rats: a rapid in vivo screening method for nanotoxicity. Toxicol Appl Pharmacol 232:292–301
25. Lewinski NA, Zhu H, Ouyang CR, Conner GP, Wagner DS, Colvin VL, Drezek RA (2011) Trophic transfer of amphiphilic polymer coated CdSe/ZnS quantum dots to Danio rerio. Nanoscale 3:3080
26. Lin D, Ji H, Tian J, Liu X, Yang N, Wu K, Wang F, Z.,2009. Environmental behavior and toxicity of engineered nanomaterials. Science in China Press. 3590–3604
27. Liu P, Duan WL, Wang QS, Li X (2010) The envelope damage of Tetrahymena in the presence of TiO_2 combined with UV light. Photochemistry Photobiology 86(3):633–638
28. Liu Z, Yu P, Cai M, Wu D, Zhang M, Huang Y, Zhao Y (2019) Polystyrene nanoplastic exposure induces immobilization, reproduction, and stress defense in the freshwater cladoceran Daphnia pulex. Chemosphere. 251(2019),74–81
29. Liu Z, Huang Y, Yang J, Chen Q, Wu D, Yu P, Li Y, Cai M, Zhao Y (2020) Polystyrene nanoplastic induces ROS production and affects the MAPK-HIF-1/NFkB-mediated antioxidant system in Daphnia pulex. Aquatic Toxicology. 220(2020),105420
30. Lohse SE, Murphy CJ (2012) Applications of Colloidal Inorganic Nanoparticles: From Medicine to Energy. Journal of the American chemical society 134:15607–15620
31. Lv Y (2019) A study on the cytotoxity of two types of nanoparticles on ciliated protozoa Pseudourostyla cristata. East China Normal University

32. Manusadzianas L, Caillet C, Fachetti L, Gylyte B, Grigutyte R, Jurkoniene S, Karitonas R, Sadauskas K, Thomas F, Vitkus R, Ferard JF (2012) Toxicity of copper oxide nanoparticle suspensions to aquatic biota. Environ Toxicol Chem. 31, 108 – 14
33. Midander K, Cronholm P, Karlsson HL, Elihn K, Möller L, Leygraf C, Wallinder IO (2009) Surface Characteristics, Copper Release, and Toxicity of Nano- and Micrometer-Sized Copper and Copper(II) Oxide Particles: A Cross-Disciplinary Study. Small 5:389–399
34. Nadtochenko VA, Rincon AG, Stanca SE, Kiwi J (2005) Dynamics of E-coli membrane cell peroxidation during TiO_2 photocatalysis studied by ATR-FTIR spectroscopy and AFM microscopy. Journal of Photochemistry Photobiology A-Chemistry 169:131–137
35. Nadtochenko V, Denisov N, Sarkisov O, Gumy D, Pulgarin C, Kiwi J (2006) Laser kinetic spectroscopy of the interfacial charge transfer between membrane cell walls of E. coli and TiO_2. Journal of Photochemistry Photobiology A: Chemistry 181:401–407
36. Ostaszewska T, Chojnacki M, Kamaszewski M, Sawosz-Chwalibog E (2016) Histopathological effects of silver and copper nanoparticles on the epidermis, gills, and liver of Siberian sturgeon. Environ Sci Pollut Res Int 23:1621–1633
37. Patterson DJ (1992) Free-living freshwater protozoa: A Color Guide [Paperback]. John Wiley & Sons
38. Paul JB, David R, Stephan H, Thomas K, Heinz F, Ken D, Roel S, Vicki S, Wolfgang K, Jurgen L, Jean K, David W, Eva O (2006) The potential risks of nanomaterials: a review carried out for ECETOC part. Particle Fibre Toxicology 3(1):article 11): 11
39. Ramyadevi J, Jeyasubramanian K, Marikani A, Rajakumar G, Rahuman AA (2012) Synthesis and antimicrobial activity of copper nanoparticles. Materials Letters 71:114–116
40. Ren G, Hu D, Cheng EW, Vargas-Reus MA, Reip P, Allaker RP (2009) Characterisation of copper oxide nanoparticles for antimicrobial applications. Int J Antimicrob Agents 33:587–590
41. Ren Y (2016) A study on silver nanoparticles cytotoxicity of Euplotes aediculatus (Ciliophora, Hypotrichida). East China Normal University
42. Sankar R, Maheswari R, Karthik S, Shivashangari KS, Ravikumar V (2014) Anticancer activity of Ficus religiosa engineered copper oxide nanoparticles. Materials Science Engineering C 44:234–239
43. Sarkar A, Das J, Manna P, Sil PC (2011) Nano-copper induces oxidative stress and apoptosis in kidney via both extrinsic and intrinsic pathways. Toxicology 290:208–217
44. Siddiqui MA, Alhadlaq HA, Ahmad J, Al-Khedhairy AA, Musarrat J, Ahamed M (2013) Copper oxide nanoparticles induced mitochondria mediated apoptosis in human hepatocarcinoma cells. PLoS One 8(8):69534
45. Song L, Vijver MG, de Snoo GR, Peijnenburg WJ (2015) Assessing toxicity of copper nanoparticles across five cladoceran species. Environ Toxicol Chem 34:1863–1869
46. Tiede K, Boxall ABA, Tear SP, Lewis J, David H, Hassellov M (2008) Detection and characterization of engineered nanoparticles in food and the environment. Food Additives Contaminants Part A-Chemistry Analysis Control Exposure Risk Assessment 25:795–821

47. Vaiopoulou E, Gikas P (2012) Effects of chromium on activated sludge and on the performance of wastewater treatment plants: A review. Water Research 46:549–570
48. Waldron HA (1980) Environmental Health Criteria Occupational Environmental Medicine 37:608
49. Wang Z, Li N, Zhao J, White JC, Qu P, Xing B (2012) CuO nanoparticle interaction with human epithelial cells: cellular uptake, location, export, and genotoxicity. Chem Res Toxicol 25:1512–1521
50. Wen J, Li J (2011) Research Progress on Copper Nanomaterials. Metallic Function Materials. 55–59
51. Werlin R, Priester JH, Mielke RE, Kraemer S (2010) Biomagnification of cadmium selenide quantum dots in a simple experimental microbial food chain. Nat Nanotechnol 6(1):65–71
52. Yang J, Hu S, Rao M, Hu L, Lei H, Wu Y, Wang Y, Ke D, Xia W, Zhu CH (2017) Copper nanoparticle-induced ovarian injury, follicular atresia, apoptosis, and gene expression alterations in female rats. Int J Nanomedicine 12:5959–5971

Figures

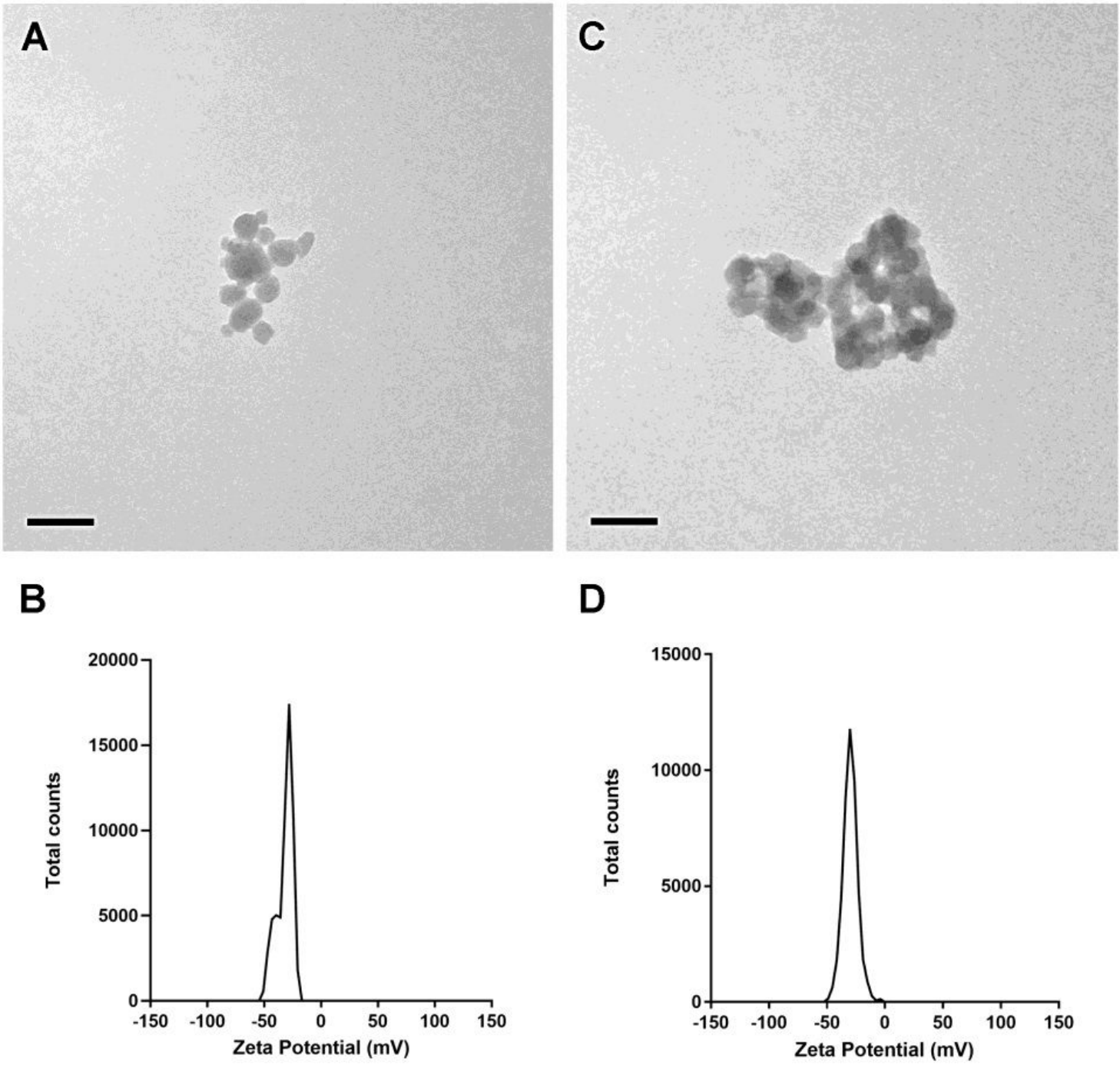

Figure 1

Characterization of CuNPs and CuONPs. Scale bars = 50 μm (AC)

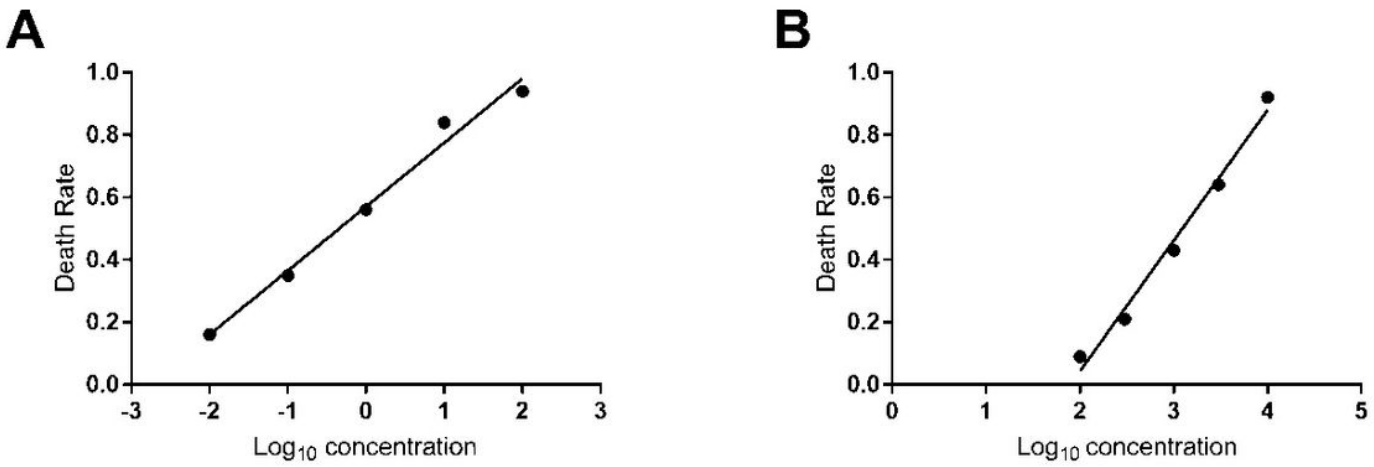

Figure 2

Regression curve of acute toxicity of CuNPs (A) and CuONPs (B) on E. aediculatus

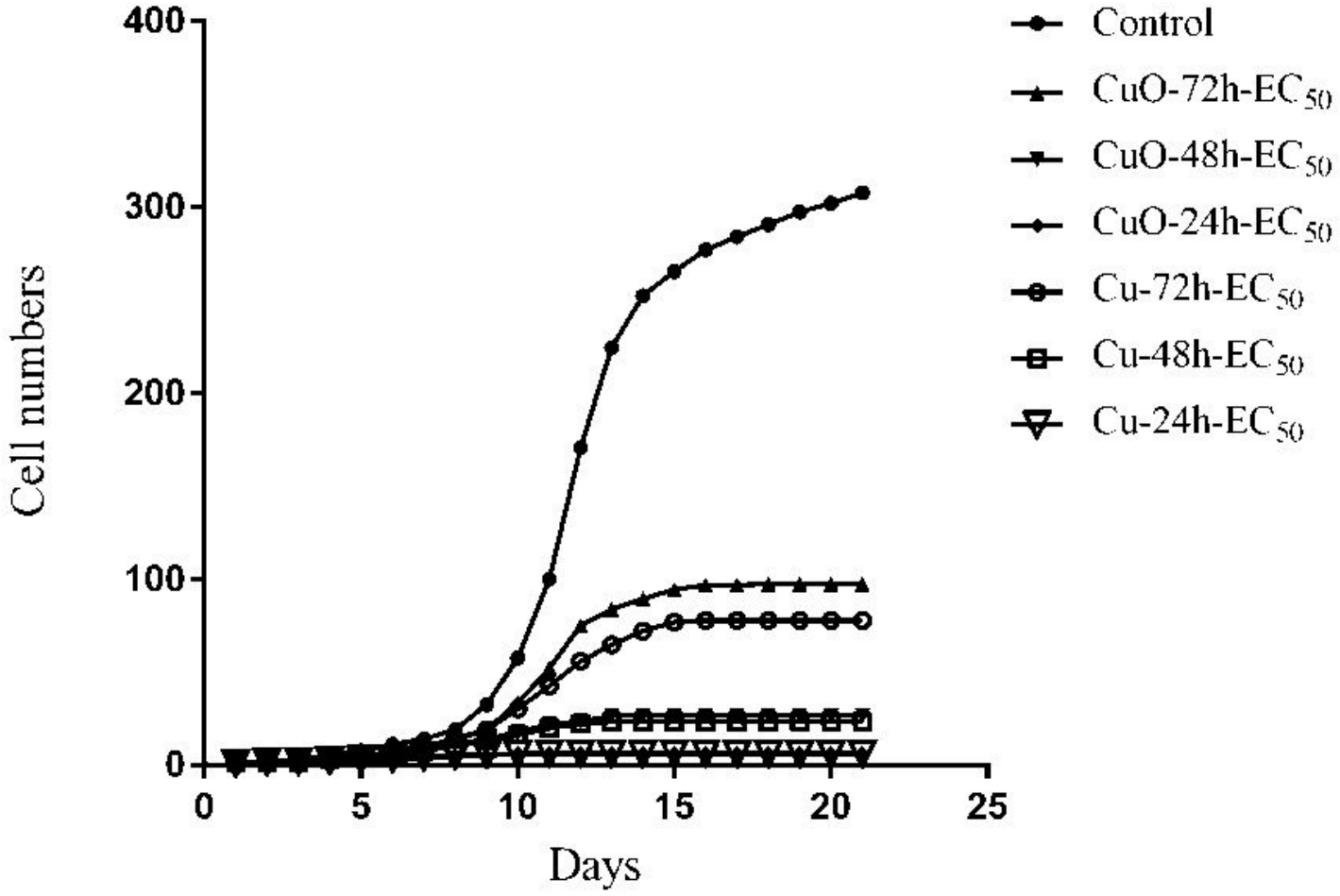

Figure 3

Inhibition curve of growth and reproduction of the two NPs on E. aediculatus

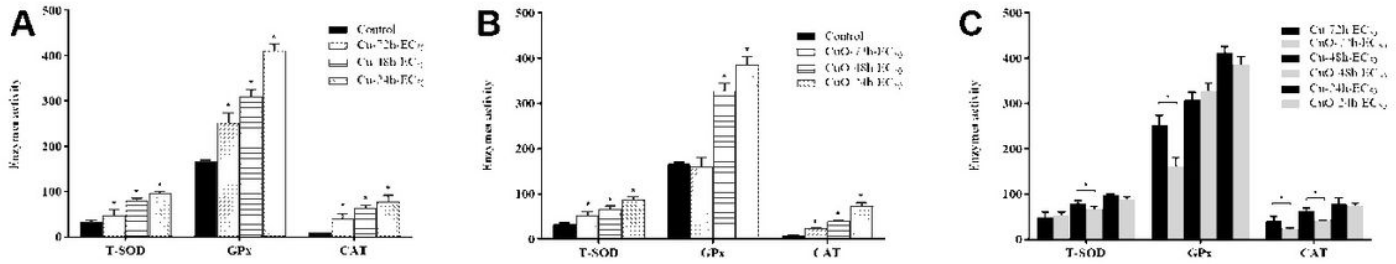

Figure 4

Enzyme activity of the two NPs on E. aediculatus

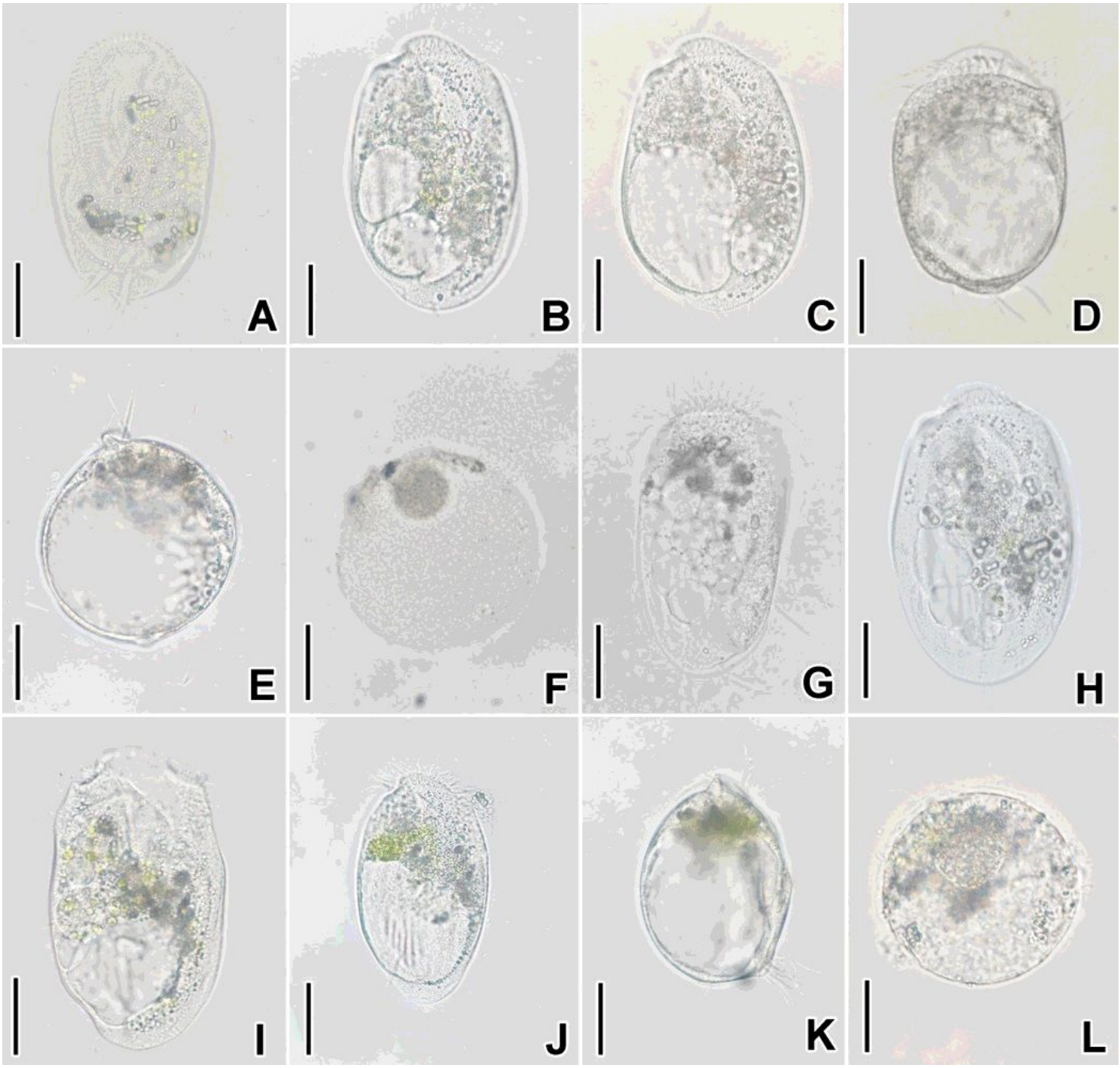

Figure 5

Observation of living cells of E. aediculatus

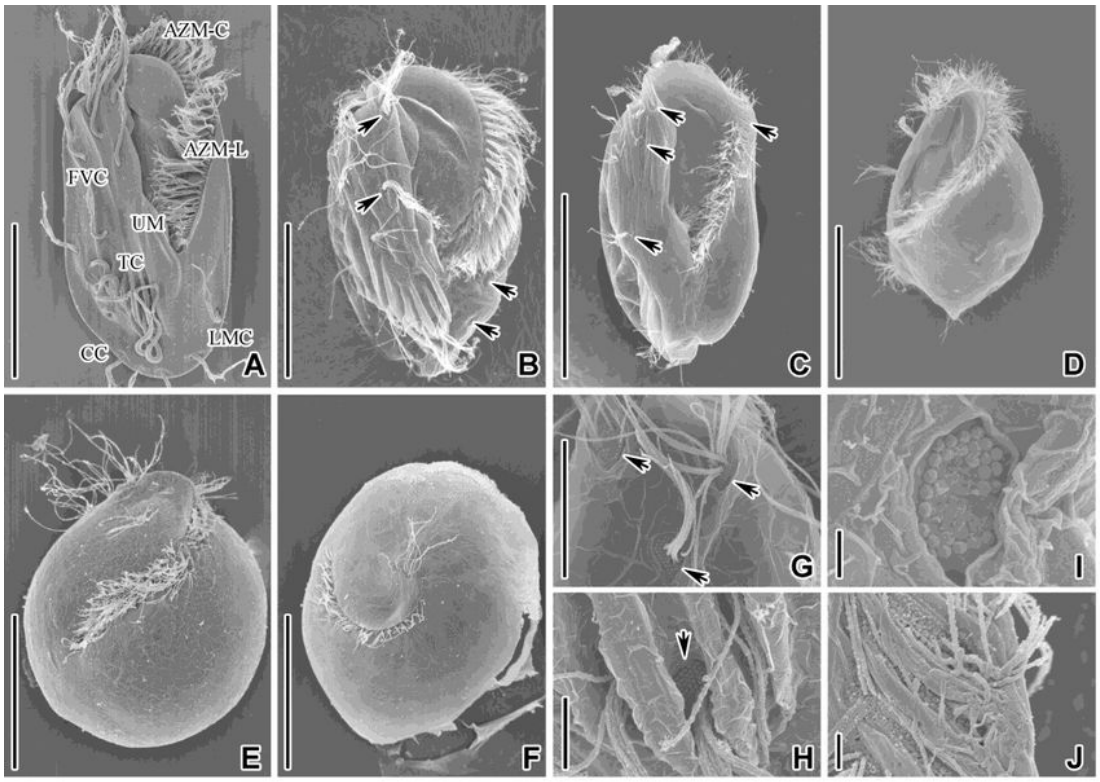

Figure 6

SEM observation of E. aediculatus from control and CuNPs group

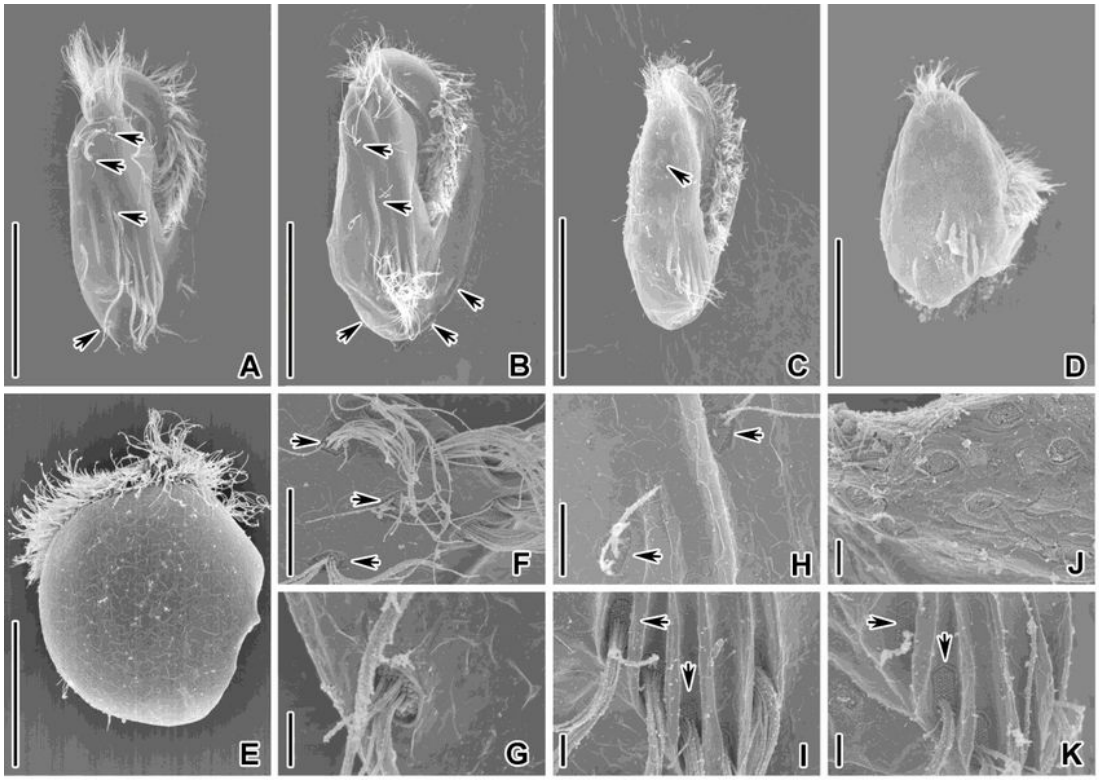

Figure 7

SEM observation of E. aediculatus from CuONPs group

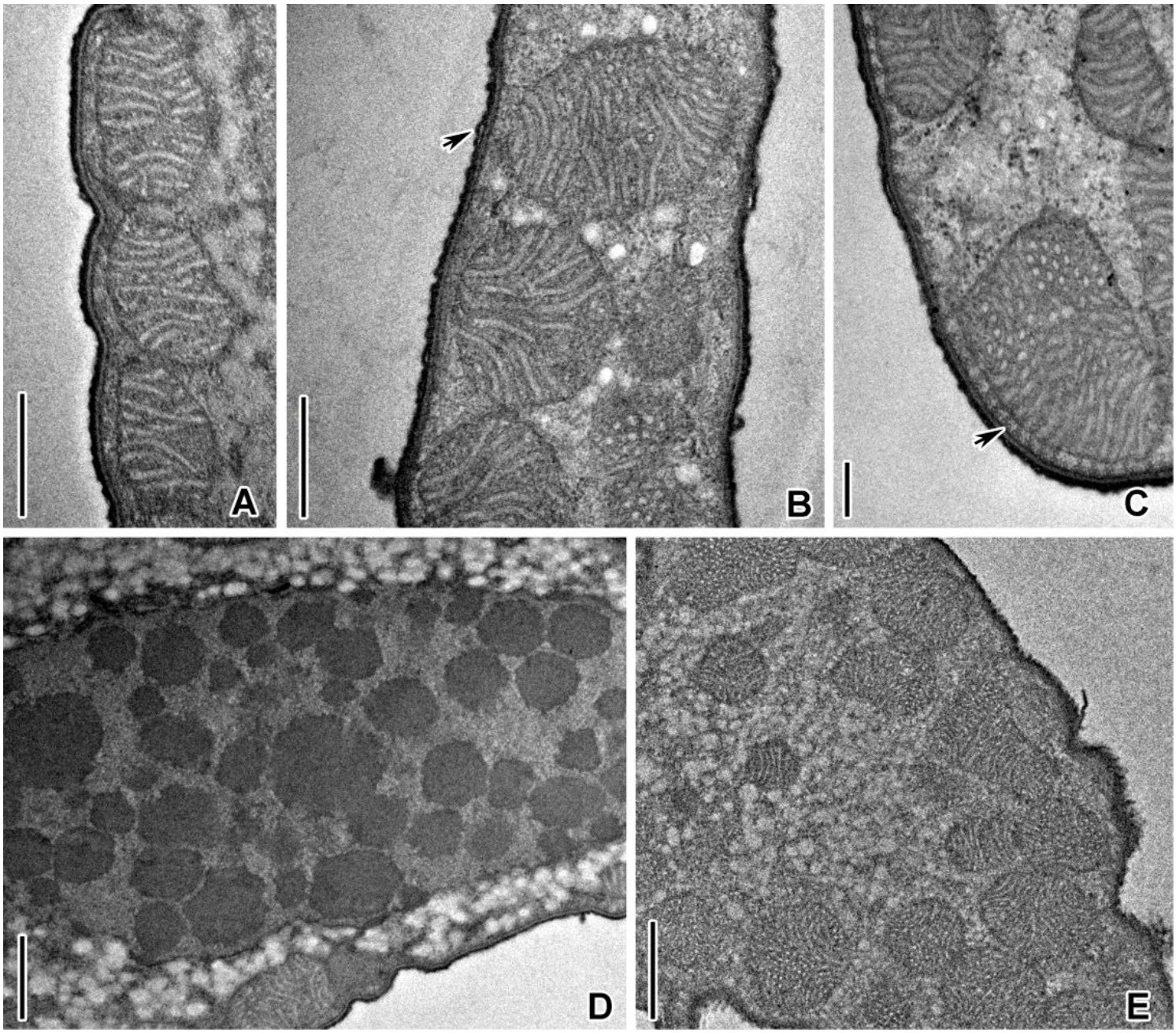

Figure 8

TEM observation of E. aediculatus from control group

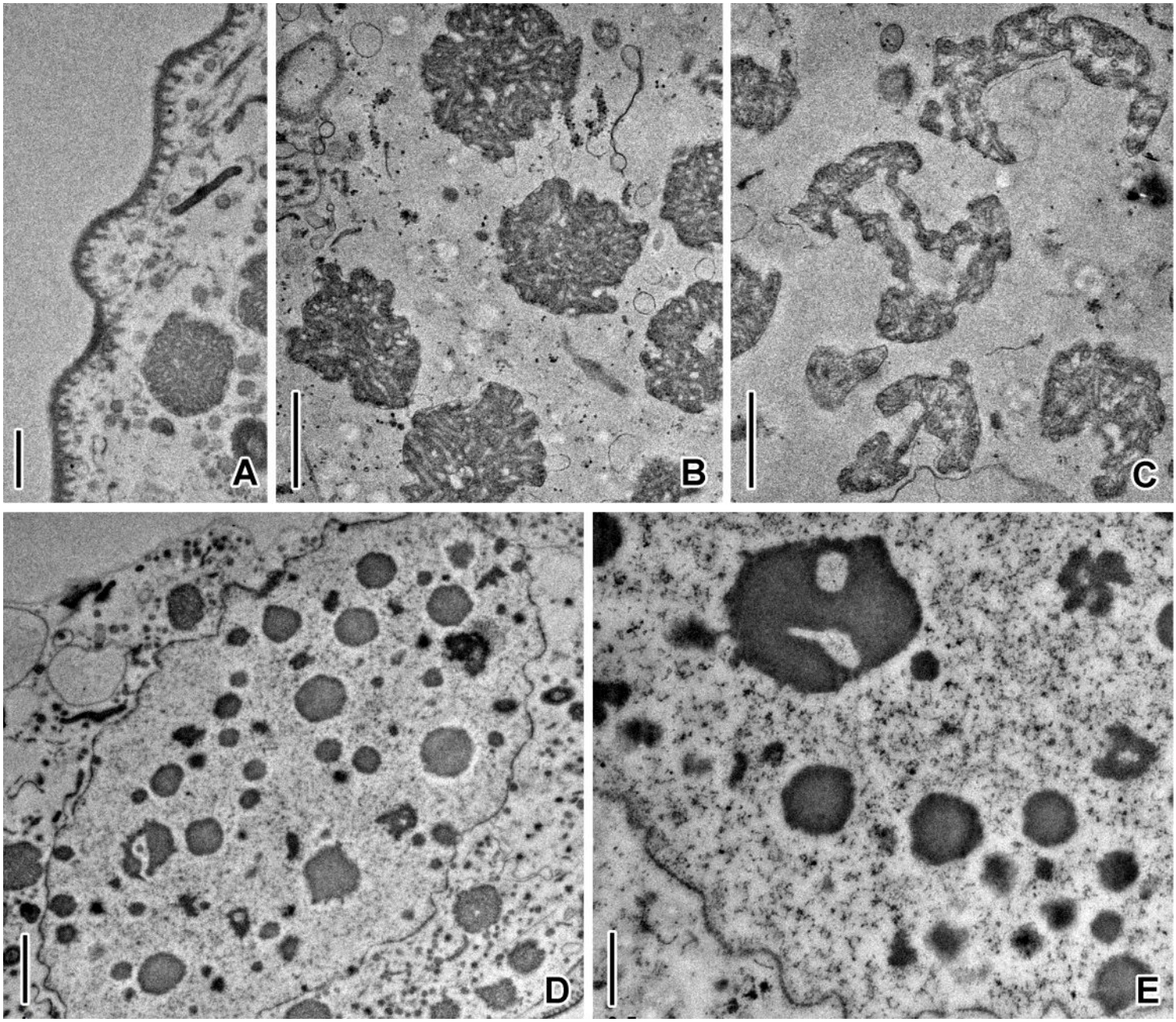

Figure 9

TEM observation of E. aediculatus from CuNPs group

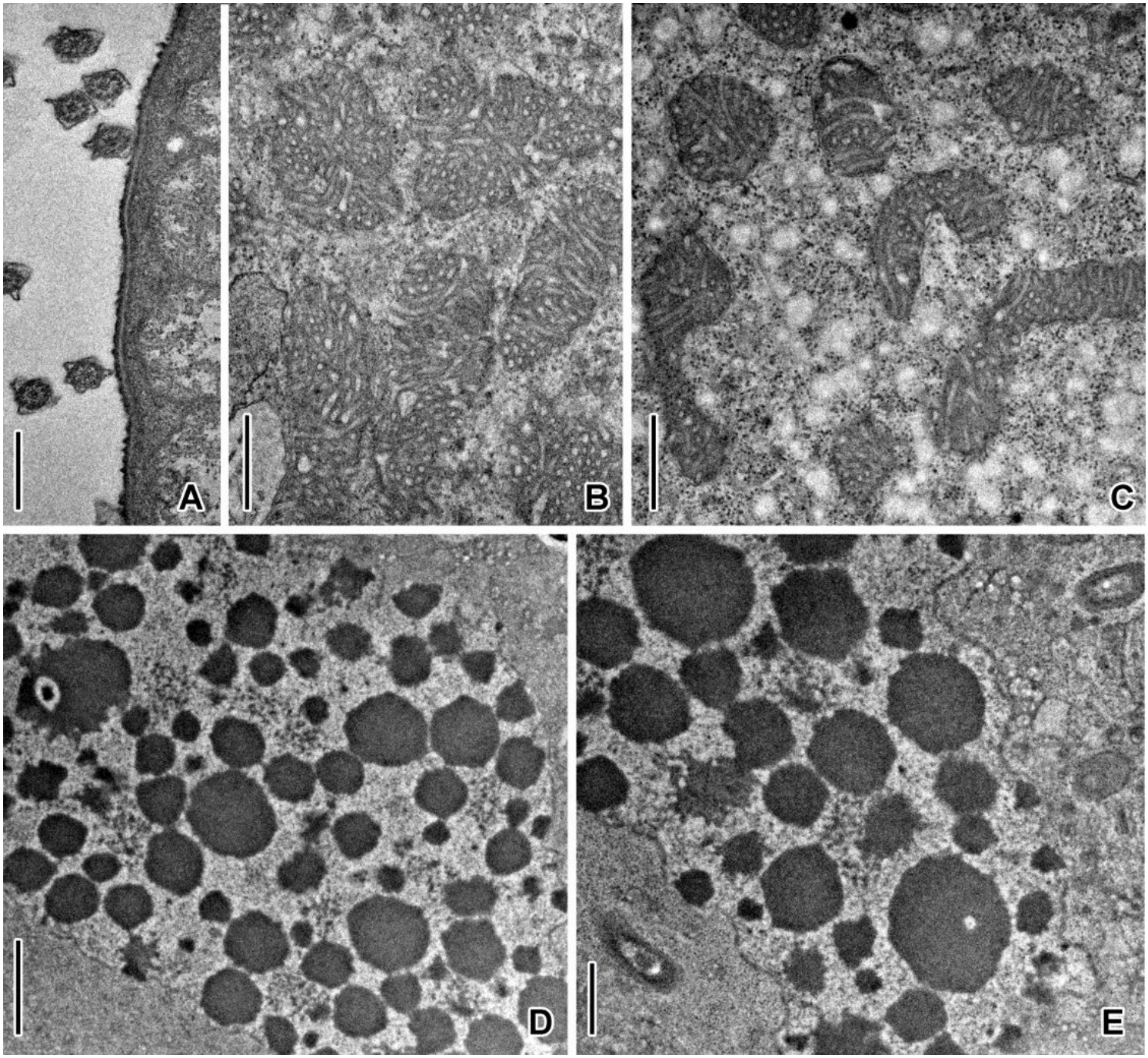

Figure 10

TEM observation of E. aediculatus from CuONPs group

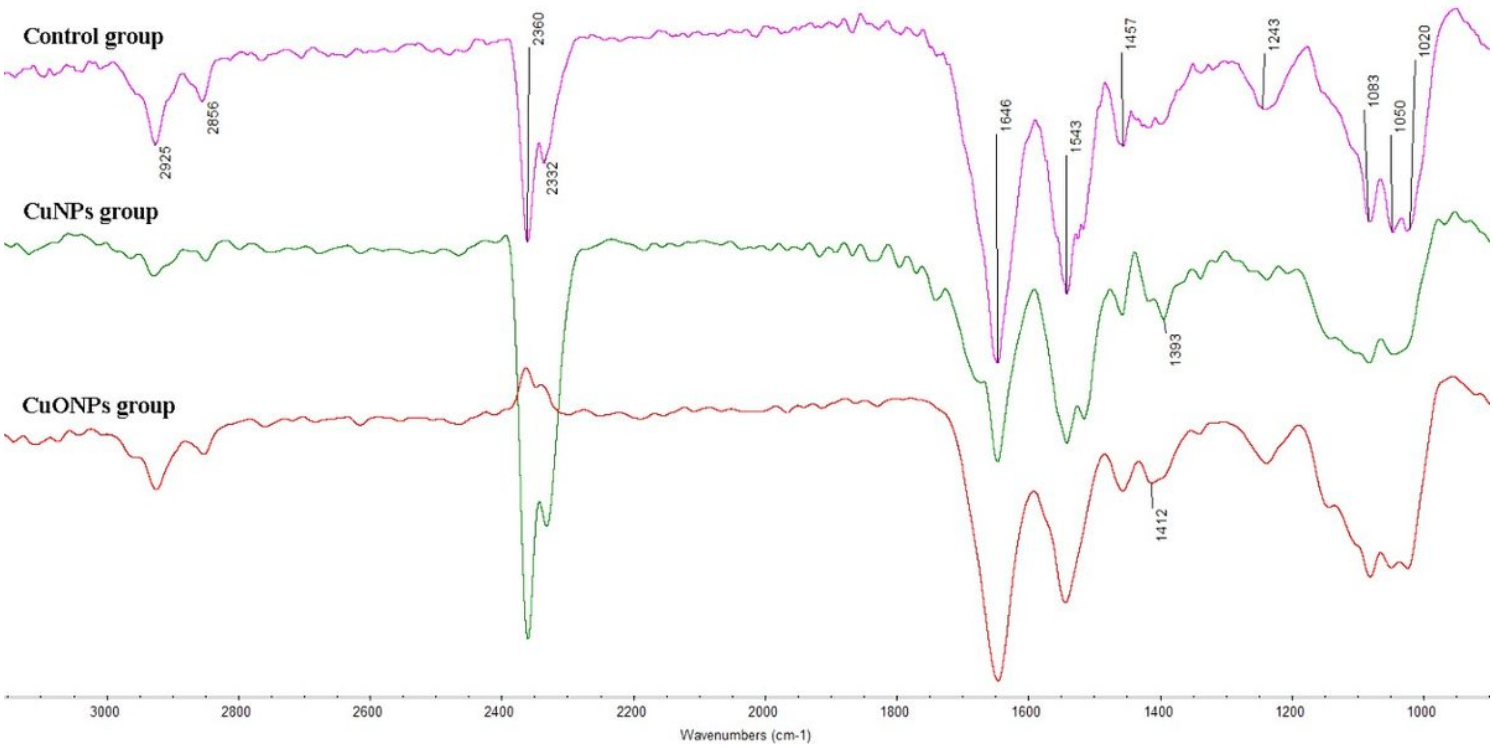

Figure 11

Fourier infrared spectra of E. aediculatus